

Two-step purification of tag-free norovirus-like particles from silkworm larvae (*Bombyx mori*)

メタデータ	言語: eng 出版者: 公開日: 2021-12-15 キーワード (Ja): キーワード (En): 作成者: Boonyakida, Jirayu, Utomo, Doddy Irawan Setyo, Soma, Fahmida Nasrin, Park, Enoch Y. メールアドレス: 所属:
URL	http://hdl.handle.net/10297/00028475

**Two-step purification of tag-free norovirus-like particles from
silkworm larvae (*Bombyx mori*)**

Short running title: Expression and purification of norovirus-like particles from
silkworm

Jirayu Boonyakida¹, Doddy Irawan Setyo Utomo¹, Fahmida Nasrin Soma², Enoch Y. Park^{1,2,*}

¹ *Department of Bioscience, Graduate School of Science and Technology, Shizuoka University,
836 Ohya, Suruga-ku, Shizuoka 422-8529, Japan*

² *Research Institute of Green Science and Technology, Shizuoka University, 836 Ohya, Suruga-
ku, Shizuoka 422-8529, Japan*

* Corresponding author.

E-mail address: park.enoch@shizuoka.ac.jp (E.Y. Park).

ABSTRACT

Recombinantly expressed VP1 of norovirus self-assembled and formed norovirus-like particles (NoV-LPs). This native VP1 was expressed using the *Bombyx mori* nucleopolyhedrovirus (BmNPV) expression system in silkworm larva. NoV-LPs were collected from silkworm fat body lysate by density gradient centrifugation. To improve the purity of the NoV-LP, the proteins were further purified using immobilized metal affinity chromatography based on the surface exposed side chain of histidine residues. The additional purification led to a highly purified virus-like particle (VLP). The morphology and size of the purified VLPs were examined using a transmission electron microscope, and dynamic light scattering revealed a monodispersed spherical morphology with a diameter of 34 nm. The purified product had a purity of >90% with a recovery yield of 54.4% (equivalent to 930 µg) from crude lysate, obtained from seven silkworm larvae. In addition, the purified VLP could be recognized by antibodies against GII norovirus in sandwich enzyme-linked immunosorbent assay, which indicated that the silkworm-derived VLP is biologically functional as a NoV-LP in its native state, is structurally correct, and exerts its biological function. Our results suggest that the silkworm-derived NoV-LP may be useful for subsequent applications, such as in a vaccine platform. Moreover, the silkworm-based expression system is known for its robustness, facile up-scalability, and relatively low expense compared to insect cell systems.

Keyword: Norovirus; Virus-like particle; Silkworm; Purification

1. Introduction

Noroviruses (NoVs) are a major cause of acute viral gastroenteritis in all age groups worldwide and generally spreads through an orofecal route [1, 2]. NoVs are non-enveloped viruses with 7.5–7.7 kb single-stranded positive-sense RNA (+ssRNA) as genetic material and belong to the family *Caliciviridae*, genus *Norovirus*. Recent phylogenetic analysis further classified NoVs into 10 genogroups (GI to GX), with at least 49 genotypes in total [3]. Of GI, GII, and GIV, which are known to infect humans, GII (particularly genotype 4 or GII.4) is the most common strain in outbreaks [1]. The NoV virion comprises two structural proteins: VP1 as a major capsid protein and VP2 as a minor capsid protein; however, VP2 is not required for particle formation [4]. Heterologous expression of VP1 alone leads to the self-assembly of a virus-like particle (VLP). The norovirus-like particle (NoV-LP) possesses an icosahedral symmetry of $T = 3$ of 90 VP1 dimers or 180 VP1 monomers with an empty capsid of approximately 30–40 nm in diameter [5, 6]. Additionally, recent studies revealed that some GII.4 NoV-LPs may exhibit polymorphic assembly of $T = 1$, $T = 3$, and $T = 4$ icosahedral symmetry [5, 7, 8].

The baculovirus expression vector system (BEVS) is a well-known protein expression system that is widely used to produce eukaryotic proteins as well as VLPs [9, 10]. Thus far, the ovarian-derived cell line of *Spodoptera frugiperda* (Sf9) and egg-derived cell line of *Trichoplusia ni* (Tn5, also known as the High Five™ cell line) are the most common commercially available systems [11]. Although the Tn5 cell line was developed to overcome the Sf9 cell line in terms of expression level [12], both systems share the same disadvantage, which is the requirement of a high-cost culture medium that serves as a challenge for scaling up protein production in insect cells. Another BEVS is the *Bombyx mori* nucleopolyhedrovirus (BmNPV)-silkworm (*B. mori*) larvae/pupae system. The use of silkworm larvae/pupae may reduce the cost, as the price per larva/pupa is

generally cheap. In addition, the silkworm-based system offers a more flexible workflow and several advantages, such as high protein production capacity, ease of upscaling, simplicity, and low risk of contamination [13–15]. Due to these attractive advantages, silkworms have been used recently to develop drugs and vaccines as a host, including VLPs [16–18].

Despite all these advantages, the system is challenged by several bottlenecks, e.g., the production of recombinant viruses, silkworm rearing schedules, and the purification procedure for VLPs, the latter of which was reviewed elsewhere by our group [16]. To solve the former, we planned to generate the recombinant BmNPV in Bm5 cells while the 4th instar silkworm larvae were developing into 5th instar larvae. The first progeny (P1) of BmNPV was then infected into silkworm at the second day of the 5th instar larvae for protein expression. This whole procedure, including gene cloning and bacmid preparation, could take approximately 2–3 weeks [17]. Protein purification from a silkworm matrix is still a major setback, and tags are often used for purification [19–22]. These studies demonstrated that host cell proteins were co-purified with target proteins even when the Ni-NTA column was applied for purification; hence, another round of purification was usually required to yield a highly purified protein.

Despite the lack of a robust cell culture system for the proliferation of norovirus, the studies related to norovirus virus have been based on the use of NoV-LP [23]. The VLP has been used to measure the antibodies that inhibit the binding of VLP to histo-blood group antigens (HBGAs) as a surrogate assay instead of a direct viral neutralization assay [24]. Additionally, NoV-LPs have been applied for the study of particle behavior in the presence of surfactants, conformation changes over a range of temperatures and pH levels, and as a VLP-based vaccine agent [25–27]. Thus far, several expression platforms have been used to develop NoV-LPs, such as Sf9 cells [28–30], *E. coli* [31], *Pichia pastoris* [32], plants [33–35], and a cell-free protein synthesis system [36].

However, none of the reported platforms utilized a silkworm-based expression system to produce GII.4 NoV-LP, for which purification is the major challenge. In this study, we constructed a recombinant BmNPV bacmid harboring norovirus VP1 and used silkworm larvae as a bioreactor to produce NoV-LPs. The VLPs were purified from a fat body that is a hard-to-purify matrix when using a two-step purification method without a purification tag.

2. Materials and Methods

2.1. Cloning of the tag-free norovirus GII.4 VP1

The full-length VP1 gene for the norovirus GII.4 Tokyo strain (GenBank accession number: BAV93798.1) was cloned into pFastBac-1 (Thermo Fisher Scientific, Tokyo, Japan) and allowed for plasmid propagation in *Escherichia coli* DH5 α . The plasmid was designated as pFB-VP1. Positive clones were selected for plasmid extraction and were sequenced to obtain the correct sequence. The plasmid was then transformed into *E. coli* BmDH10bac (CP⁻ Chi⁻) [37] for bacmid generations, then plated onto LB agar supplemented with 50 μ g/ml kanamycin, 7 μ g/ml gentamycin, 10 μ g/ml tetracycline, 0.5 mM 5-bromo-4-chloro-3-indolyl- β -d-galactopyranoside (X-Gal), and 0.25 mM isopropyl β -d-1-thiogalactopyranoside (IPTG) for blue/white colony selection [33]. The recombinant bacmid prepared from the white colony was designated as “rBmNPV CP⁻ Chi⁻/VP1 bacmid.”

2.2. Expression of GII.4 NoV-LPs

The recombinant bacmid harboring the VP1 gene (rBmNPV CP⁻ Chi⁻/VP1 bacmid) was transfected into *Bombyx mori* cell lines (Bm5). After 5 d of incubation, the culture medium was collected and used as a recombinant virus stock (rBmNPV CP⁻ Chi⁻/VP1 virus). The recovered baculovirus was employed for infecting the fifth instar silkworm larvae (Ehime Sansyu, Ehime, Japan) [38]. The silkworms were reared in a controlled environment at 26°C with relative humidity at 70%–85% and were fed an artificial diet (Silkmate S2, Nosan Co., Yokohama, Japan). The fat body was collected, and a hemolymph was drawn from the larvae at 5 d post-infection (dpi). The fat body was resuspended in Tris-buffered saline (TBS, pH 7.6) containing 0.1% Triton X-100, sonicated (30% amplitude, 15 s on/off, 15 cycles) (ultrasonic homogenizer LUH150, Yamato Scientific, Tokyo, Japan), centrifuged (10,000 × g, 15 min, 4°C), and filtered through a 0.45 µm nitrocellulose filter (Merck, Tokyo, Japan), then stored at –80°C until use. The hemolymph was mixed with an anti-melanogenesis agent, 1-phenyl-2-thiourea, at a final concentration of 2.5 mM immediately after drawing and was stored at –80°C as a virus stock for further infection.

Two analytical methods were used to examine the expression level of VP1 in silkworm. First, western blot analysis was employed to compare the fat body lysate (soluble fraction) against the known concentration of purified VP1. Second, using Quantity One Imaging software (Bio-Rad), the amount of purified protein was calculated based on a band percentage after separation on sodium dodecyl sulfate-polyacrylamide gel electrophoresis (SDS-PAGE) gel followed by Coomassie Brilliant Blue (CBB) staining to measure the total protein.

2.3. Purification

2.3.1. First step: Sucrose gradient centrifugation of tag-free GIL4 NoV-LPs

To purify the VLPs, the soluble fraction of fat body lysate was subjected to sucrose gradient centrifugation. First, the VLPs were concentrated by ultracentrifugation at $122,000 \times g$ for 1 h at 4°C using an S52-ST swinging-bucket rotor by overlaying the fat body lysate on a 30% sucrose cushion. Then, the VLPs were further purified via a discontinuous sucrose density gradient centrifugation at $122,000 \times g$ for 3 h at 4°C using the same rotor by overlaying the concentrated sample on 20%, 30%, 40%, 50%, and 60% (w/v) sucrose cushions. Sucrose residue was removed from the VLP suspension by overnight dialysis against phosphate buffered saline (PBS) at pH 7.4 with a dialysis membrane of size 20 (MWCO 14,000 Da) (Wako, Tokyo, Japan).

2.3.2. Second step: Immobilized metal affinity chromatography of tag-free GII.4 NoV-LPs

After dialysis, chromatographic purification of the VLPs was performed. The VLP suspension was filtered through a 0.22 µm nitrocellulose filter (Merck, Tokyo, Japan) prior to injecting a HisTrap HP 5 mL column (GE Healthcare, Tokyo, Japan), which was connected to a Biologic DuoFlow chromatography system (Bio-Rad, Tokyo, Japan). The loaded column was washed with five column volumes (CV) of a washing buffer (20 mM NaH₂PO₄, 0.5 M NaCl, 10 mM imidazole, pH 7.4) before being eluted with a step gradient consisting of 100 mM (5 CV), 250 mM (5 CV), 500 mM (5 CV), and 1 M (10 CV) imidazole in a washing buffer. The flow rate of load/injection of the sample was 0.2 mL/min to allow more time for the VLPs to interact with the Ni²⁺-nitrilotriacetic acid (NI-NTA), while the flow rate for the remaining steps was 1 mL/min. After IMAC purification of the VLPs, fractions containing the target protein were combined and dialyzed overnight against PBS (pH 7.4) prior to subsequent experiments.

2.4. SDS-PAGE and western blot analysis

Each protein sample was mixed with an equal volume of 2× sodium dodecyl sulfate (SDS) loading buffer (0.125 M of Tris-HCl pH 6.8, 4% w/v of SDS, 20% v/v of glycerol, 0.01% of bromophenol blue, and 0.01% w/v of 2-mercaptoethanol) and heated at 100°C. Samples were separated on 12% SDS-polyacrylamide gels and stained with CBB before transfer to the polyvinylidene difluoride membrane (Merck, Tokyo, Japan). After transfer, the membrane was blocked with 5% (w/v) skim milk (Wako, Tokyo, Japan) in TBS + 0.1% Tween 20 (TBS-T) followed by anti-NoV-VP1 (NS14) mouse monoclonal antibody (mAb) [39] as a primary antibody and horseradish peroxidase (HRP)-conjugated anti-mouse IgG (MBL, Tokyo, Japan) as a secondary antibody. The specific protein bands were visualized by applying Immobilon Western Chemiluminescent HRP substrate (Merck, Tokyo, Japan) on the membrane.

2.5. Transmission electron microscopy and dynamic light scattering

The integrity of VLPs was confirmed via transmission electron microscopy (TEM; JEM-1400Flash, JEOL Ltd., Akishima Tokyo, Japan). VLP suspensions at a 1 mg/mL final concentration were applied on a copper grid (Nisshin EM, Tokyo, Japan). The grid was allowed to absorb a VLP suspension for 30 min at room temperature, which was washed three times with a filter-sterilized PBS and stained with 1% phosphotungstic acid for 2 min. The grid was dried overnight inside a desiccator chamber. The TEM images were acquired on JEOL JEM-1400Flash TEM.

The size distribution of VLPs was measured by dynamic light scattering (DLS) using Zetasizer Nano ZS (Malvern Panalytical Ltd., Malvern, UK), following a technique described by Brié et al.

[40]. Diameters of the VLPs were obtained from two independent experiments, with each hydrodynamic diameter measurement performed in triplicate.

2.6. Sandwich enzyme-linked immunosorbent assay

In addition to TEM and DLS analysis, the double-antibody sandwich enzyme-linked immunosorbent assay (ELISA) with a NV-EIA Kit (Denka Seiken, Tokyo, Japan) was performed to determine the tentative biological function of NoV-LPs. In brief, the concentration of purified VLPs was adjusted to 0.5 mg/mL in PBS (pH 7.4) then diluted 1:10 until 1:500,000. The diluted samples were added to an anti-GII mouse mAb pre-coated plate and incubated at 27°C for 40 min. After washing the wells three times with the provided washing buffer, HRP-conjugated anti-GII type 104 rabbit polyclonal antibody (pAb) was added to each well, incubated at 27°C for 20 min, and washed. After washing, the HRP substrate was added to the wells, which was maintained at 27°C for 15 min before adding a stop solution (0.3 M sulfuric acid). The absorbance was measured at 450 nm, and the background was subtracted at 655 nm.

2.7. Protein analysis

After ultracentrifugation and Ni-NTA purification, the concentrations of total protein in the soluble fraction of fat body lysate were determined via Bradford's Protein Assay Kit (Bio-Rad, Tokyo, Japan) in a 96-well microtiter plate according to the manufacturer's protocol. The assay was performed in duplicate, and the absorbance was measured at 595 nm.

Protein purities and band intensities after ultracentrifugation and Ni-NTA purification were determined using a densitometry tool in Quantity One (Bio-Rad). Proteins were first separated on

a 12% SDS-PAGE gel, then stained with CBB. The gel was imaged and converted into a 16-bit grayscale TIFF file before being opened in Quantity One. In the program, the bands were detected at a high sensitivity to detect faint bands, and the background was subtracted at a disk size of 25 mm. The percentage purity after Ni-NTA purification was defined as the Band %, whereas the purity of the target protein after ultracentrifugation was defined as [(Band % of the target protein in lane “ultracentrifugation”/Band % of the target protein in land “IMAC”) × 100].

2.8 DNA assay for nucleic acid impurity reduction

To measure the nucleic acid reduction after each purification, a Qubit dsDNA BR Assay Kit (Thermo Scientific, Tokyo, Japan) was used according to the manufacturer’s protocol. The assay was performed in a 96-well microtiter plate. The fluorescence at 485/530 nm (excitation/emission) was measured using an Infinite M Plex (Tecan, Kanagawa, Japan). The assay was performed in duplicate.

3. Results

3.1. Expression of NoV-LPs using silkworm larvae

The expression of norovirus VP1 was investigated at 5 dpi using rBmNPV/VP1 via SDS-PAGE and western blot analysis. As there was no secretion signal peptide [41] on the VP1 construct, the VP1 protein was expected to be primarily expressed and accumulated in fat bodies. As expected, the VP1 protein was mainly detected in the fat body as a soluble form (Figs. 1A and B) with a size of approximately 55 kDa. The expression amount of VP1 in silkworm larvae was

determined by western blot analysis of the silkworm fat body lysate in comparison with the purified VP1 and by using Quantity One software. By western blot analysis, the expression amount was 159 $\mu\text{g/mL}$ (Fig. 1B). In this study, 12 mL of the soluble fraction of fat body lysate was obtained from seven larvae; therefore, productivity was 272 $\mu\text{g VP1/larvae}$ as a soluble protein. Using the Quantity One software for analysis, the VP1 band proportion was approximately 6.1% of the total proteins. Total protein measured by Bradford's assay was 33.41 mg; therefore, the VP1 amount corresponded to be approximately 2.04 mg of the total protein or 291 $\mu\text{g/larvae}$ of a soluble VP1 protein. These two results obtained from two different analytical methods were in good agreement.

3.2. The first step of purification: Sucrose gradient centrifugation

The fat body lysate collected from rBmNPV/VP1-infected silkworm larvae at 5 dpi was subjected to sucrose gradient centrifugation, which is a powerful method for separating subcellular particles, including viruses, based on the sedimentation coefficient of the particles [42]. Thus, this method was applied to separate the VLPs from most of the host cell proteins (HCPs) as a pretreatment step. The VP1 protein was observed in fractions 6–10 and in some remaining impurities below the target protein, while most HCPs were removed from the suspension (Fig. 2A). These fractions were then combined and dialyzed overnight against PBS (pH 7.4). At this step, the purity of VLP was approximately 78% (Band %: 71.4), and the recovery of VP1 was 61.2% (Table 1). After ultracentrifugation, the sample was observed under negative-staining TEM. VLPs with good uniformity were observed (Fig. 2B, white arrows). However, the image suffered from impurities that were co-purified through centrifugation.

232

233 *3.3. The second step of purification: Chromatographic purification of VLPs*

234 Although the majority of HCPs were removed from the VLP by ultracentrifugation, some
235 remaining host proteins required an additional method of separation to meet the requirement of a
236 pharmaceutical grade product. To remove the remaining HCPs, the Ni-NTA column or His-tagged
237 affinity column was employed to further improve the quality and purity of the VLP. After dialysis,
238 the VLP suspension was applied to a Ni-NTA column, washed, and eluted from the column (Fig.
239 3). The chromatographic profile revealed that there were some unbound proteins in the
240 flowthrough, whereas little to no proteins were found in the washing fraction. Bound proteins were
241 eluted from the column when imidazole increased from 10 mM to 100 mM, and the highest A₂₈₀
242 peak was obtained at 250 mM imidazole (Fig. 3A). The fractions were then analyzed by SDS-
243 PAGE, which revealed that some of the VP1 protein failed to bind to the column and remained in
244 the flowthrough with contaminant proteins. In the washing fraction, a small amount of VP1 protein
245 was removed from the column. In the elution fraction, most of the contaminant proteins were
246 removed from the target protein (Fig. 3B). After Ni-NTA purification, an improvement in the
247 purity of the VP1 protein was noticeable when compared to the purified product after
248 ultracentrifugation (Fig. 3C). The eluents containing VP1 protein were combined and dialyzed
249 against PBS (pH 7.4) prior to subsequent analyses. The purity of the VLPs improved to more than
250 90% (Band %: 91.5%), as determined by Quantity One imaging software after the second
251 purification, with an approximate 48.7% recovery of VP1 (Fig. 3C and Table 1).

252

253 *3.4. DNA reduction*

Besides removing impurity proteins, reduction of DNA after each step of purifications was also determined (Table 1). The total DNA in the starting material was 392.89 μg and was reduced to 13.06 μg with a 96.7% reduction after the first purification step. The host DNA was further reduced to 1.78 μg at 86.37% reduction of the second step. Through two-step purification, the DNA amount in the purified VP1 was reduced up to 99.55%.

3.5 Characterization of Ni-purified silkworm-derived VLP/VP1

DLS analysis revealed that the Ni-NTA purified VLP/VP1s had an approximated diameter of 34 nm (Fig. 4A), which could be observed under TEM with good uniformity (Fig. 4B). These results indicated that most of the silkworm-derived VP1 could form homogeneous particles with a size of 34 nm in diameter. The biological function of silkworm-derived GII.4 VLP was tested by the recognition of anti-GII mAb as a capture antibody and reactive anti-GII type 104 rabbit pAb as a detection antibody in a sandwich ELISA (Fig. 5A). The binding of most antibodies is influenced by conformation epitopes at the native state of antigens, particularly mAbs, which target only one epitope, while pAbs can target both conformational epitopes and linear epitopes on antigens [43, 44]. Thus, the detection of virus particles through sandwich ELISA using mAb (capture antibody), which was expected to have an affinity toward a conformational epitope, and pAb (detection antibody), which could target both linear and conformational epitopes, depends on the conformation and antigen–antibody interaction. The sandwich ELISA confirmed the presence of VLPs, a conformation of the VLP, and accessibility for antibodies in their native state (Fig. 5B). From this result, the silkworm-derived GII.4 VLP was recognized as NoV-LPs.

4. Discussion

The silkworm-based expression system has been known as a “bioreactor” for producing foreign proteins, and the expression levels are superior to insect cell systems. However, protein purification from silkworm lysate is still a significant setback [16]. Protein tags are often required for the purification of proteins from silkworm compartments [19–22]. Intact human papillomavirus (HPV) 6b L1-VLPs could be isolated from a fat body of silkworm larvae using heparin affinity chromatography, but with many HCPs [45]. A study demonstrated the use of silkworm pupae to produce Nakayama-VLP (NVLP), which was purified via sucrose gradient centrifugation; however, some HCPs still remained in the purified product [46]. Several studies used silkworm-BEVS as a platform for producing rabbit hemorrhagic disease virus-like particles (RHDV-VLPs), porcine parvovirus-like particles (PPV-VLPs), and canine parvovirus-like particles (CPV-VLPs). These VLPs were separated from fat bodies by a single round of ammonium sulfate precipitation, but the purity of the purified products was not discussed [47–49]. Porcine circovirus type 2 (PCV2) VLPs purified from silkworm pupae by an ammonium sulfate precipitation (as a first step) and anion exchange chromatography (as a second step) resulted in ~90% purity [14]. These studies suggest the need for second step purification to obtain highly purified VLPs from silkworm compartments for downstream experiments, especially in the vaccinology field. In this study, we demonstrated the use of a silkworm-based expression system to produce NoV-LP and purified them from a fat body compartment.

Several protein expression platforms have been applied for the production of NoV-LP e.g., *E. coli*, yeasts, insect cells, plants, and a cell-free system. The yield of NoV-LPs produced by *E. coli*-based system was reported to be about 1.5–3 mg of a soluble GST-fusion protein per one liter culture (mg/L) [50]. Several reports had applied the transgenic plant *Nicotiana benthamiana* for

production of GII.4 NoV-LP and the productivity was approximately 1 mg/g leaf weight [33, 35]. However, the use of a plant-based system could be hampered by disadvantages including the risk of transgene contamination, low expression level, and time-consuming genetic manipulation procedures [51]. A higher yield could be achieved when applying the insect cell-based system (Sf9) of over 0.1 g/L [52]. Recently, the *P. pastoris* and *E. coli*-based CFPS systems have been employed for producing NoV-LPs. Both systems could produce NoV-LPs at high yields (0.6 g/L from *P. pastoris* and 1 g/L from CFPS) [36, 53]. However, these systems share the same disadvantage of a relatively high production cost which might obstruct the upscaling process. Further, the protein production in *P. pastoris* requires methanol which is proven to be difficult to control the optimum level of methanol during the protein induction step and may experience proteolytic digestion of the target protein [54]. Silkworm is known for its' high capacity in producing recombinant proteins including VLPs, ease of scaling up, cost-efficient, and easier of management with a simple workflow. In here, we applied silkworm *B. mori* larvae for NoV-LP preparation and the yield was about 0.27 mg/larva. Our result demonstrated that a milligram order of NoV-LP can be obtained in a matter of days.

Our recent study attempted to purify VP1 from a silkworm fat body compartment by using nickel magnetic nanoparticles (Ni-MNPs). The result revealed that nearly half of HCPs retained the target protein, thus signifying that silkworms contain numerous histidine-rich proteins or nickel-binding proteins [55]. We suggested in a recent study that using the His-affinity technique is useful for pretreatment before injection into the chromatographic system or may be useful after a pretreatment step for the purification of His-tagged protein from a silkworm matrix. Although there are several pretreatment methods, such as cesium chloride (CsCl) density gradient centrifugation and polyethylene glycol (PEG) precipitation, both may interfere with downstream

experiments [56]. Therefore, the approach was to use sucrose gradient centrifugation as the first step and the Ni-NTA column as the second step. The first step was aimed to collect, concentrate, and separate the NoV-LPs from fat body lysates, and the second step was to improve the purity of the VLPs.

Despite comprehensive studies on the preparation and production of NoV-LP, the methods used in such studies have usually relied upon centrifugation and PEG precipitation [30, 35, 56]. Several studies have applied chromatographic purification for NoV-LP preparation, e.g., an anion exchange chromatography after PEG precipitation [28]; ammonium sulfate precipitation and chromatographic columns (size exclusion chromatography [SEC] column, CHT™ column, or a hydrophobic interaction chromatography [Me-HIC] column) [31, 57]; or an Ni-NTA (IMAC) column for His-tagged NoV-LP [29] or a tag-free NoV-LP from *P. pastoris* before SEC [32]). Although the Ni-NTA column has been applied as a first step for purification, the result indicates that GII.4 NoV-LPs can bind to the column even without a histidine tag.

Prior to the use of an Ni-NTA column, we tried to purify the NoV-LP using an SEC column after ultracentrifugation. However, the protein was lost during the run, and the loss was higher than 95% in our experience (Supplementary Information, Figs. 1A and B). The low recovery was probably due to non-ideal interactions of the target protein with the column matrix [58, 59]. The SEC result imposed upon us the need to seek an alternative method, and Ni-NTA was a promising choice. Thus, silkworm-derived NoV-LPs were applied to the Ni-NTA column, washed with 10 mM imidazole buffer, and eluted with a stepwise protocol. We noticed that there were some VP1 proteins and impurities in the flowthrough, whereas were little to no VP1/NoV-LPs in the washing. The NoV-LPs began to elute from the column when the imidazole concentration was 100 mM, whereas most of the target was eluted at 250 mM imidazole. The ability to bind to the Ni-NTA

matrix of NoV-LP was attributed to the histidine residues exposed on the natural surface of each VP1 monomer, which were synergized with adjacent tryptophan, tyrosine, or phenylalanine residues [32, 60]. Throughout these steps, the obtained NoV-LPs showed decent purity and excellent uniformity with a size of approximately 34–37 nm in diameter. The sandwich ELISA showed a good response against the silkworm-derived NoV-LP, which indicated that the VLPs had correct folding and conformation in their native state and were primed for a subsequent application.

In addition, removal of the host cell DNA was analyzed after each step of purification. There is a concern that DNA impurity may pose product safety issues, such as coprecipitation and increased fluid viscosity, as told by the Food and Drug Administration and the World Health Organization. The DNA content was reduced by 96.7% after the first step of ultracentrifugation and by more than 99.5% after the second step of purification.

5. Conclusion

In this study, we employed silkworm larvae as a protein expression platform for tag-free norovirus VP1. Each silkworm has a capability to produce the VP1 protein of 270 µg/larva. The expression of VP1 led to self-assembly into VLPs and mainly accumulated in the fat body compartment. The VLPs were purified by a two-step purification procedure consisting of a sucrose gradient centrifugation to concentrate the VLPs from fat body lysates as the first step and IMAC or Ni-NTA chromatographic affinity as the second step to trap the VLPs based on the high density of histidine residues on the surface of each particle. The purified VLPs were observed under TEM, and the tentative biological function was determined by a sandwich ELISA, by which NoV-LPs

could be identified. Through these steps, we were able to obtain NoV-LPs with a purity of more than 90%. A final protein yield was ~0.93 mg from seven silkworm larvae, which was equivalent to 48.7% of VP1 recovery from the starting material. Hence, mass production of NoV-LP could be achieved with the use of a silkworm-based expression system.

Declaration of competing interest

The authors declare that there is no conflict of interest.

Funding

This work has been funded by the Japan Society for the Promotion of Science (JSPS) KAKENHI Grant-in-Aid for Scientific Research (A) (Grant No. 20H00411).

Acknowledgment

We would like to acknowledge Prof. Tetsuro Suzuki of Hamamatsu University School of Medicine for providing us the anti-NoV mouse mAb (NS14) as a courtesy gift for our studies. This work was funded by the JSPS KAKENHI Grant-in-Aid for Scientific Research (A) No. 20H00411.

Author contributions

Jirayu Boonyakida conducted the experiments and wrote the draft manuscript. Doddy Irawan Setyo Utomo performed supportive experiments. Fahmida Nasrin Soma operated on the TEM

imaging system. Jirayu Boonyakida and Enoch Y. Park conceived and designed the study. Enoch Y. Park reviewed and edited the manuscript.

References

- [1] R.I. Glass, U.D. Parashar, M.K. Estes, Norovirus gastroenteritis. *N. Engl. J. Med.*, 361 (2009) 1776–1785.
- [2] L.G. Thorne, I.G. Goodfellow, Norovirus gene expression and replication. *J. Gen. Virol.*, 95 (2014) 278–291.
- [3] P. Chhabra, M. de Graaf, G.I. Parra, M.C.-W. Chan, K. Green, V. Martella, Q. Wang, P.A. White, K. Katayama, H. Vennema, M.P.G. Koopmans, J. Vinjé, Updated classification of norovirus genogroups and genotypes. *J. Gen. Virol.*, 100 (2019) 1393–1406.
- [4] A. Bertolotti-Ciarlet, L.J. White, R. Chen, B.V.V. Prasad, M.K. Estes, Structural requirements for the assembly of norwalk virus-like particles. *J. Virol.*, 76 (2002) 4044–4055.
- [5] J.M. Devant, G.S. Hansman, Structural heterogeneity of a human norovirus vaccine candidate. *Virology*, 553 (2021) 23–34.
- [6] R. Pogan, J. Dülfer, C. Uetrecht, Norovirus assembly and stability. *Curr. Opin. Virol.*, 31 (2018) 59–65.
- [7] J.M. Devant, G. Hofhaus, D. Bhella, G.S. Hansman, Heterologous expression of human norovirus GII.4 VP1 leads to assembly of T=4 virus-like particles. *Antiviral. Res.*, 168 (2019) 175–182.
- [8] J. Jung, T. Grant, D.R. Thomas, C.W. Diehnelt, N. Grigorieff, L. Joshua-Tor, High-resolution cryo-EM structures of outbreak strain human norovirus shells reveal size variations. *Proc. Natl. Acad. Sci.*, 116 (2019) 12828.

410 [9] A.C. Chambers, M. Aksular, L.P. Graves, S.L. Irons, R.D. Possee, L.A. King, Overview
411 of the baculovirus expression system. *Curr. Protoc. Protein. Sci.*, 91 (2018) 5.4.1–5.4.6.

412 [10] F. Liu, X. Wu, L. Li, Z. Liu, Z. Wang, Use of baculovirus expression system for generation
413 of virus-like particles: Successes and challenges. *Protein Expr. Purif.*, 90 (2013) 104–116.

414 [11] X. Zhou, H. Bai, M. Kataoka, M. Ito, M. Muramatsu, T. Suzuki, T.-C. Li, Characterization
415 of the self-assembly of New Jersey polyomavirus VP1 into virus-like particles and the virus
416 seroprevalence in Japan. *Sci. Rep.*, 9 (2019) 13085.

417 [12] T.R. Davis, T.J. Wickham, K.A. McKenna, R.R. Granados, M.L. Shuler, H.A. Wood,
418 Comparative recombinant protein production of eight insect cell lines. *In Vitro Cell. Dev. Biol.*
419 *Anim.*, 29 (1993) 388–390.

420 [13] L. Yao, S. Wang, S. Su, N. Yao, J. He, L. Peng, J. Sun, Construction of a baculovirus-
421 silkworm multigene expression system and its application on producing virus-like particles. *PLoS*
422 *One*, 7 (2012) e32510.

423 [14] A. Masuda, J.M. Lee, T. Miyata, T. Sato, S. Hayashi, M. Hino, D. Morokuma, N. Karasaki,
424 H. Mon, T. Kusakabe, Purification and characterization of immunogenic recombinant virus-like
425 particles of porcine circovirus type 2 expressed in silkworm pupae. *J. Gen. Virol.*, 99 (2018) 917–
426 926.

427 [15] T.A. Kost, J.P. Condey, D.L. Jarvis, Baculovirus as versatile vectors for protein
428 expression in insect and mammalian cells. *Nat. Biotechnol.*, 23 (2005) 567–575.

429 [16] R. Minkner, E.Y. Park, Purification of virus-like particles (VLPs) expressed in the
430 silkworm *Bombyx mori*. *Biotechnol. Lett.*, 40 (2018) 659–666.

431 [17] T. Kato, M. Kajikawa, K. Maenaka, E.Y. Park, Silkworm expression system as a platform
432 technology in life science. *Appl. Microbiol. Biotechnol.*, 85 (2010) 459–470.

433 [18] M. Kajikawa, K. Sasaki-Tabata, H. Fukuhara, M. Horiuchi, Y. Okabe, Silkworm
434 baculovirus expression system for molecular medicine. *J. Biotechnol. Biomater.*, S9 (2012) 005.

435 [19] R. Fujita, M. Hino, T. Ebihara, T. Nagasato, A. Masuda, J.M. Lee, T. Fujii, H. Mon, K.
436 Kakino, R. Nagai, M. Tanaka, Y. Tonooka, T. Moriyama, T. Kusakabe, Efficient production of
437 recombinant SARS-CoV-2 spike protein using the baculovirus-silkworm system. *Biochem.*
438 *Biophys. Res. Commun.*, 529 (2020) 257–262.

439 [20] D. Morokuma, J. Xu, M. Hino, H. Mon, J.S. Merzaban, M. Takahashi, T. Kusakabe, J.M.
440 Lee, Expression and characterization of human β -1, 4-galactosyltransferase 1 (β 4GalT1) using
441 silkworm–baculovirus expression system. *Mol. Biotechnol.*, 59 (2017) 151–158.

442 [21] A.S. Al-Amoodi, K. Sakashita, A.J. Ali, R. Zhou, J.M. Lee, M. Tehseen, M. Li, J.C.I.
443 Belmonte, T. Kusakabe, J.S. Merzaban, Using eukaryotic expression systems to generate human
444 α 1,3-fucosyltransferases that effectively create selectin-binding glycans on stem cells.
445 *Biochemistry*, 59 (2020) 3757–3771.

446 [22] Y. Morifuji, J. Xu, N. Karasaki, K. Iiyama, D. Morokuma, M. Hino, A. Masuda, T. Yano,
447 H. Mon, T. Kusakabe, J.M. Lee, Expression, purification, and characterization of recombinant
448 human α 1-antitrypsin produced using silkworm–baculovirus expression system. *Mol. Biotechnol.*,
449 60 (2018) 924–934.

450 [23] M. de Graaf, J. van Beek, M.P.G. Koopmans, Human norovirus transmission and evolution
451 in a changing world. *Nat. Rev. Microbiol.*, 14 (2016) 421–433.

452 [24] L.C. Lindesmith, M.T. Ferris, C.W. Mullan, J. Ferreira, K. Debbink, J. Swanstrom, C.
453 Richardson, R.R. Goodwin, F. Baehner, P.M. Mendelman, R.F. Bargatze, R.S. Baric, Broad
454 Blockade Antibody Responses in Human Volunteers after Immunization with a Multivalent

455 Norovirus VLP Candidate Vaccine: Immunological Analyses from a Phase I Clinical Trial. PLoS
 456 Med., 12 (2015) e1001807.

457 [25] B.S. Mertens, O.D. Velez, Characterization and control of surfactant-mediated Norovirus
 458 interactions. Soft Matter, 11 (2015) 8621–8631.

459 [26] R. Pogan, C. Schneider, R. Reimer, G. Hansman, C. Uetrecht, Norovirus-like VP1 particles
 460 exhibit isolate dependent stability profiles. J. Phys. Condens. Matter, 30 (2018) 064006.

461 [27] S. Esposito, N. Principi, Norovirus Vaccine: Priorities for Future Research and
 462 Development. Front. Immunol., 11 (2020).

463 [28] T. Koho, T. Mäntylä, P. Laurinmäki, L. Huhti, S.J. Butcher, T. Vesikari, M.S. Kulomaa,
 464 V.P. Hytönen, Purification of norovirus-like particles (VLPs) by ion exchange chromatography. J.
 465 Virol. Methods, 181 (2012) 6–11.

466 [29] T. Koho, T.O. Ihalainen, M. Stark, H. Uusi-Kerttula, R. Wieneke, R. Rahikainen, V.
 467 Blazevic, V. Marjomäki, R. Tampé, M.S. Kulomaa, V.P. Hytönen, His-tagged norovirus-like
 468 particles: A versatile platform for cellular delivery and surface display. Eur. J. Pharm. Biopharm.,
 469 96 (2015) 22–31.

470 [30] Y. Huo, X. Wan, T. Ling, J. Wu, Z. Wang, S. Meng, S. Shen, Prevailing Sydney like
 471 Norovirus GII.4 VLPs induce systemic and mucosal immune responses in mice. Mol. Immunol.,
 472 68 (2015) 367–372.

473 [31] Y. Huo, X. Wan, T. Ling, J. Wu, W. Wang, S. Shen, Expression and purification of
 474 norovirus virus like particles in *Escherichia coli* and their immunogenicity in mice. Mol. Immunol.,
 475 93 (2018) 278–284.

476 [32] Y.-L. Chen, C.-T. Huang, Establishment of a two-step purification scheme for tag-free
 477 recombinant Taiwan native norovirus P and VP1 proteins. J. Chromatogr. B, 1159 (2020) 122357.

478 [33] A.G. Damos, H.S. Mason, High-level expression and enrichment of norovirus virus-like
479 particles in plants using modified geminiviral vectors. *Protein Expr. Purif.*, 151 (2018) 86–92.

480 [34] L.G. Mathew, M.M. Herbst-Kralovetz, H.S. Mason, Norovirus Narita 104 virus-like
481 particles expressed in *Nicotiana benthamiana* induce serum and mucosal immune responses.
482 *Biomed. Res. Int.*, 2014 (2014) 807539.

483 [35] L. Santi, L. Batchelor, Z. Huang, B. Hjelm, J. Kilbourne, C.J. Arntzen, Q. Chen, H.S.
484 Mason, An efficient plant viral expression system generating orally immunogenic Norwalk virus-
485 like particles. *Vaccine*, 26 (2008) 1846–1854.

486 [36] J. Sheng, S. Lei, L. Yuan, X. Feng, Cell-free protein synthesis of norovirus virus-like
487 particles. *RSC Adv.*, 7 (2017) 28837–28840.

488 [37] E.Y. Park, T. Abe, T. Kato, Improved expression of fusion protein using a cysteine-
489 protease- and chitinase-deficient *Bombyx mori* (silkworm) multiple nucleopolyhedrovirus bacmid
490 in silkworm larvae. *Biotechnol. Appl. Biochem.*, 49 (2008) 135–140.

491 [38] T. Motohashi, T. Shimojima, T. Fukagawa, K. Maenaka, E.Y. Park, Efficient large-scale
492 protein production of larvae and pupae of silkworm by *Bombyx mori* nuclear polyhedrosis virus
493 bacmid system. *Biochem. Biophys. Res. Commun.*, 326 (2005) 564–569.

494 [39] T.D. Parker, N. Kitamoto, T. Tanaka, A.M. Hutson, M.K. Estes, Identification of
495 genogroup I and genogroup II broadly reactive epitopes on the norovirus capsid. *J. Virol.*, 79 (2005)
496 7402–7409.

497 [40] A. Brié, I. Bertrand, M. Meo, N. Boudaud, C. Gantzer, The effect of heat on the
498 physicochemical properties of bacteriophage MS2. *Food Environ. Virol.*, 8 (2016) 251–261.

499 [41] M. Futatsumori-Sugai, K. Tsumoto, Signal peptide design for improving recombinant
500 protein secretion in the baculovirus expression vector system. *Biochem. Biophys. Res. Commun.*,
501 391 (2010) 931–935.

502 [42] C.R. McEwen, Tables for estimating sedimentation through linear concentration gradients
503 of sucrose solution. *Anal. Biochem.*, 20 (1967) 114–149.

504 [43] N.S. Lipman, L.R. Jackson, L.J. Trudel, F. Weis-Garcia, Monoclonal versus polyclonal
505 antibodies: distinguishing characteristics, applications, and information resources. *ILAR J.*, 46
506 (2005) 258–268.

507 [44] B. Forsström, B. Bisławska Axnäs, J. Rockberg, H. Danielsson, A. Bohlin, M. Uhlen,
508 Dissecting antibodies with regards to linear and conformational epitopes. *PLoS One*, 10 (2015)
509 e0121673.

510 [45] M. Palaniyandi, T. Kato, E.Y. Park, Expression of human papillomavirus 6b L1 protein in
511 silkworm larvae and enhanced green fluorescent protein displaying on its virus-like particles.
512 *SpringerPlus*, 1 (2012) 29.

513 [46] S. Matsuda, R. Nerome, K. Maegawa, A. Kotaki, S. Sugita, K. Kawasaki, K. Kuroda, R.
514 Yamaguchi, T. Takasaki, K. Nerome, Development of a Japanese encephalitis virus-like particle
515 vaccine in silkworms using codon-optimised prM and envelope genes. *Heliyon*, 3 (2017) e00286.

516 [47] S.H. Lee, S.M. Bae, W.S. Gwak, S.D. Woo, Production of porcine parvovirus virus-like
517 particles using silkworm larvae. *J. Asia-Pacif. Entomol.*, 22 (2019) 1167–1172.

518 [48] X. Zheng, S. Wang, W. Zhang, X. Liu, Y. Yi, S. Yang, X. Xia, Y. Li, Z. Zhang,
519 Development of a VLP-based vaccine in silkworm pupae against rabbit hemorrhagic disease virus.
520 *Int. Immunopharmacol.*, 40 (2016) 164–169.

521 [49] H. Feng, G.-q. Hu, H.-l. Wang, M. Liang, H. Liang, H. Guo, P. Zhao, Y.-j. Yang, X.-x.
522 Zheng, Z.-f. Zhang, Y.-k. Zhao, Y.-w. Gao, S.-t. Yang, X.-z. Xia, Canine parvovirus VP2 protein
523 expressed in silkworm pupae self-assembles into virus-like particles with high immunogenicity.
524 PLoS One, 9 (2014) e79575.

525 [50] M. Tan, W. Zhong, D. Song, S. Thornton, X. Jiang, E. coli-expressed recombinant
526 norovirus capsid proteins maintain authentic antigenicity and receptor binding capability. J. Med.
527 Virol., 74 (2004) 641–649.

528 [51] M.J.B. Burnett, A.C. Burnett, Therapeutic recombinant protein production in plants:
529 Challenges and opportunities. Plants, People, Planet, 2 (2020) 121–132.

530 [52] T. Koho, L. Huhti, V. Blazevic, K. Nurminen, S.J. Butcher, P. Laurinmäki, N. Kalkkinen,
531 G. Rönnholm, T. Vesikari, V.P. Hytönen, M.S. Kulomaa, Production and characterization of virus-
532 like particles and the P domain protein of GII.4 norovirus. J. Virol. Methods, 179 (2012) 1–7.

533 [53] J. Tomé-Amat, L. Fleischer, S.A. Parker, C.L. Bardliving, C.A. Batt, Secreted production
534 of assembled Norovirus virus-like particles from *Pichia pastoris*. Microb. Cell Fact., 13 (2014) 134.

535 [54] M. Karbalaeei, S.A. Rezaee, H. Farsiani, *Pichia pastoris*: A highly successful expression
536 system for optimal synthesis of heterologous proteins. J. Cell. Physiol., 235 (2020) 5867–5881.

537 [55] R. Minkner, J. Xu, K. Takemura, J. Boonyakida, H. Wätzig, E.Y. Park, Ni-modified
538 magnetic nanoparticles for affinity purification of His-tagged proteins from the complex matrix of
539 the silkworm fat body. J. Nanobiotechnol., 18 (2020) 159.

540 [56] L. Huhti, V. Blazevic, K. Nurminen, T. Koho, V.P. Hytönen, T. Vesikari, A comparison
541 of methods for purification and concentration of norovirus GII-4 capsid virus-like particles. Arch.
542 Virol., 155 (2010) 1855–1858.

- [57] J. Kissmann, S.F. Ausar, T.R. Foubert, J. Brock, M.H. Switzer, E.J. Detzi, T.S. Vedvick, C.R. Middaugh, Physical stabilization of Norwalk virus-like particles. *J. Pharm. Sci.*, 97 (2008) 4208–4218.
- [58] T. Arakawa, D. Ejima, T. Li, J.S. Philo, The critical role of mobile phase composition in size exclusion chromatography of protein pharmaceuticals. *J. Pharm. Sci.*, 99 (2010) 1674–1692.
- [59] I.K. Ventouri, D.B.A. Malheiro, R.L.C. Voeten, S. Kok, M. Honing, G.W. Somsen, R. Haselberg, Probing protein denaturation during size-exclusion chromatography using native mass spectrometry. *Anal. Chem.*, 92 (2020) 4292–4300.
- [60] V. Gaberc-Porekar, V. Menart, Perspectives of immobilized-metal affinity chromatography. *J. Biochem. Biophys. Methods*, 49 (2001) 335–360.

Figure legends

Fig. 1. Expression of norovirus VP1 protein in silkworm larvae. **(A)** Fat bodies of rBmNPV/VP1-infected silkworm larvae at 5 dpi were collected and analyzed by SDS-PAGE followed by CBB staining and western blot analysis with mouse mAb against norovirus VP1 protein. H: hemolymph. S: soluble fraction of fat body. P: precipitate or insoluble fraction of fat body. The hashtag “#” indicates VP1 band. **(B)** Western blot analysis for the VP1 expression level in silkworm larvae. The VP1 band from a soluble fraction of silkworm larva fat body was determined by a comparison with the known concentration of purified VP1 protein. CBB: Coomassie Brilliant Blue; SDS-PAGE: sodium dodecyl sulfate–polyacrylamide gel electrophoresis

Fig. 2. First purification step. **(A)** Sucrose gradient centrifugation of expressed VP1. Fat body lysates of rBmNPV/VP1-infected silkworm containing VP1 were layered on the top of 20%–60% (w/w) discontinuous sucrose cushions and were subjected to centrifugation. Ten fractions (~500 µl/fraction) were taken from the top to bottom and analyzed by SDS-PAGE analysis. **(B)** Negative-

566 staining TEM analysis of the LP1 particles after ultracentrifugation (scale bar: 100 nm). VLPs are
567 indicated by white arrows. SDS-PAGE: sodium dodecyl sulfate–polyacrylamide gel
568 electrophoresis; TEM: transmission electron microscopy; VLP: virus-like particle

569 **Fig. 3.** Second purification step using the Ni-NTA chromatographic column (HisTrap). **(A)**
570 Chromatographic profile of VLPs on HisTrap column. **(B)** SDS-PAGE analysis of the loading (L)
571 sample, flowthrough (FT), washing (W), and elution (E) fractions. **(C)** SDS-PAGE analysis of the
572 VLP before and after each step of purification. Purities of VP1 after ultracentrifugation and after
573 IMAC (Ni-NTA) were determined using densitometry; gray indicates background intensity of each
574 lane. IMAC: Immobilized metal affinity chromatography; SDS-PAGE: sodium dodecyl sulfate–
575 polyacrylamide gel electrophoresis; VLP: virus-like particle

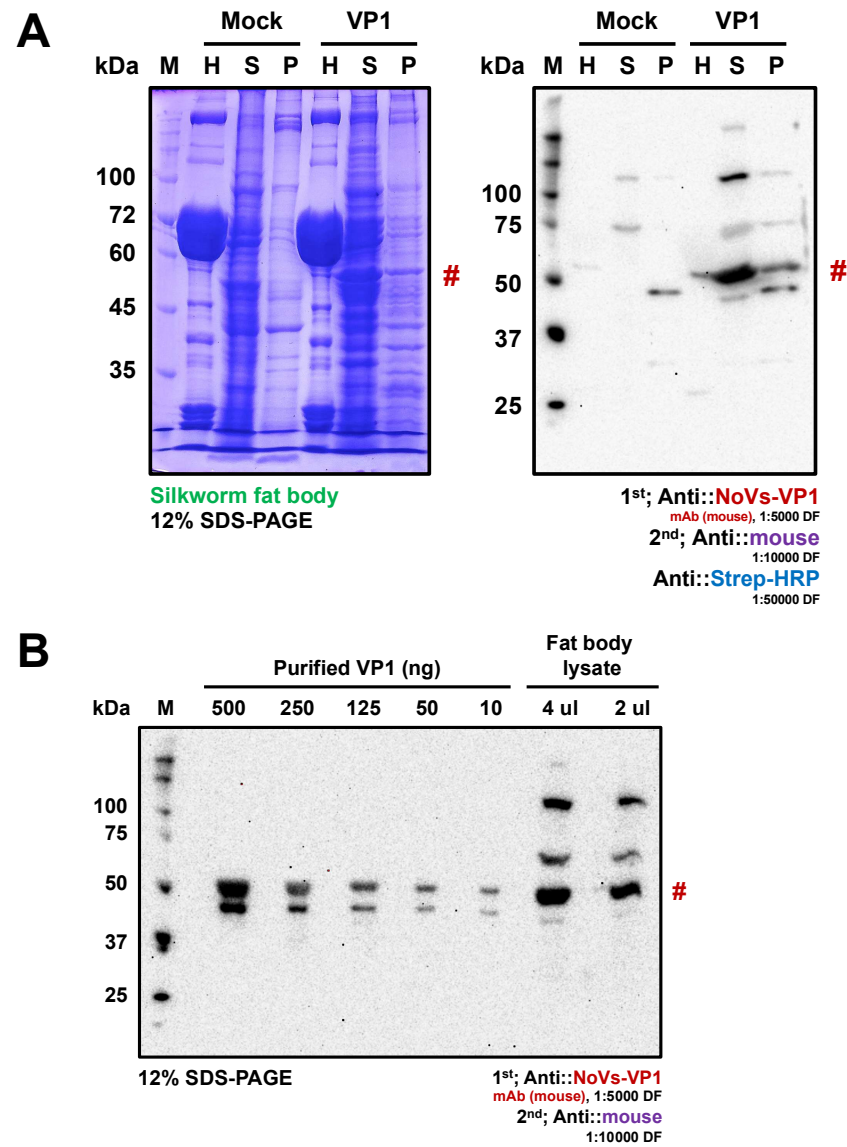
576 **Fig. 4.** Characterization of Ni-purified NoV-LP. **(A)** DLS analysis of VLP-containing pool fraction
577 after chromatographic purification. **(B)** Negative-staining TEM analysis (scale bar: 100 nm). VLP:
578 virus-like particle

579 **Fig. 5.** Sandwich ELISA for the detection of purified silkworm-derived NoV-LP. **(A)** Schematic
580 diagram of a sandwich ELISA using anti-GII type 104 rabbit pAb as a detection antibody for NoV-
581 LP. **(B)** Sandwich ELISA for the detection of the native NoV-LP.

582 **Table 1.** Tag-free NoV-LP purification summary

Sample	VP1 conc. (µg/mL)	VP1 amount (mg)	VP1 recovery (%)	Protein amount (mg)	Protein reduction (%)	Step yield (%)	Purity (%)	DNA amount (µg)	DNA reduction (%)
Fat body lysate	160	1.91	-	33.41	-	-	-	392.89	-
After ultracentrifugation	120	1.17	61.32	1.38	95.88	4.1	78	13.06	96.68
After IMAC purification	460	0.93	48.69	0.93	97.22	67.4	>90	1.78	99.55

583 IMAC: Immobilized metal affinity chromatography; NoV-LP: norovirus-like particles



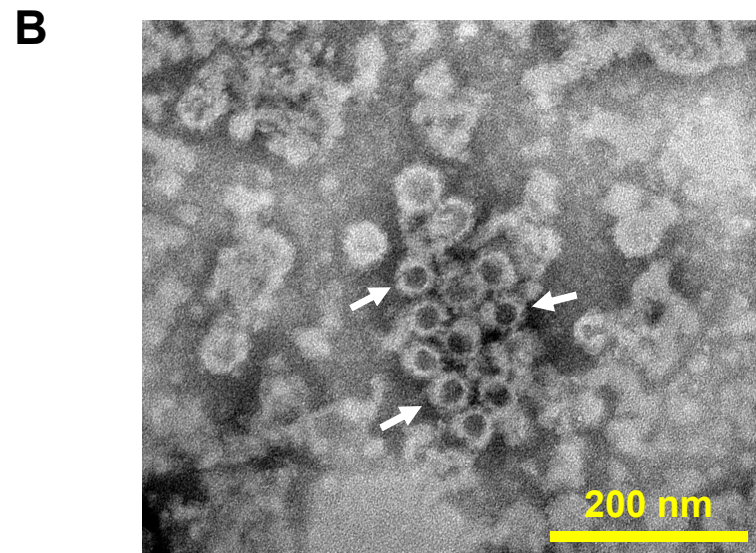
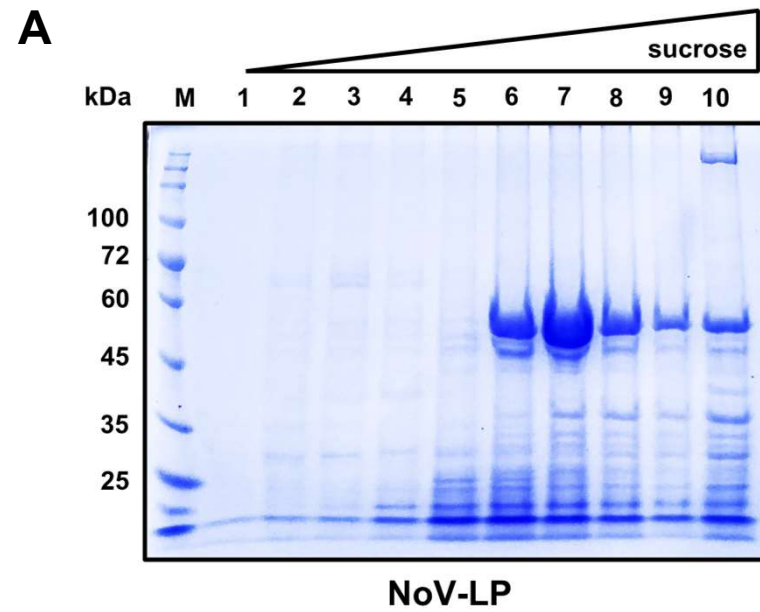
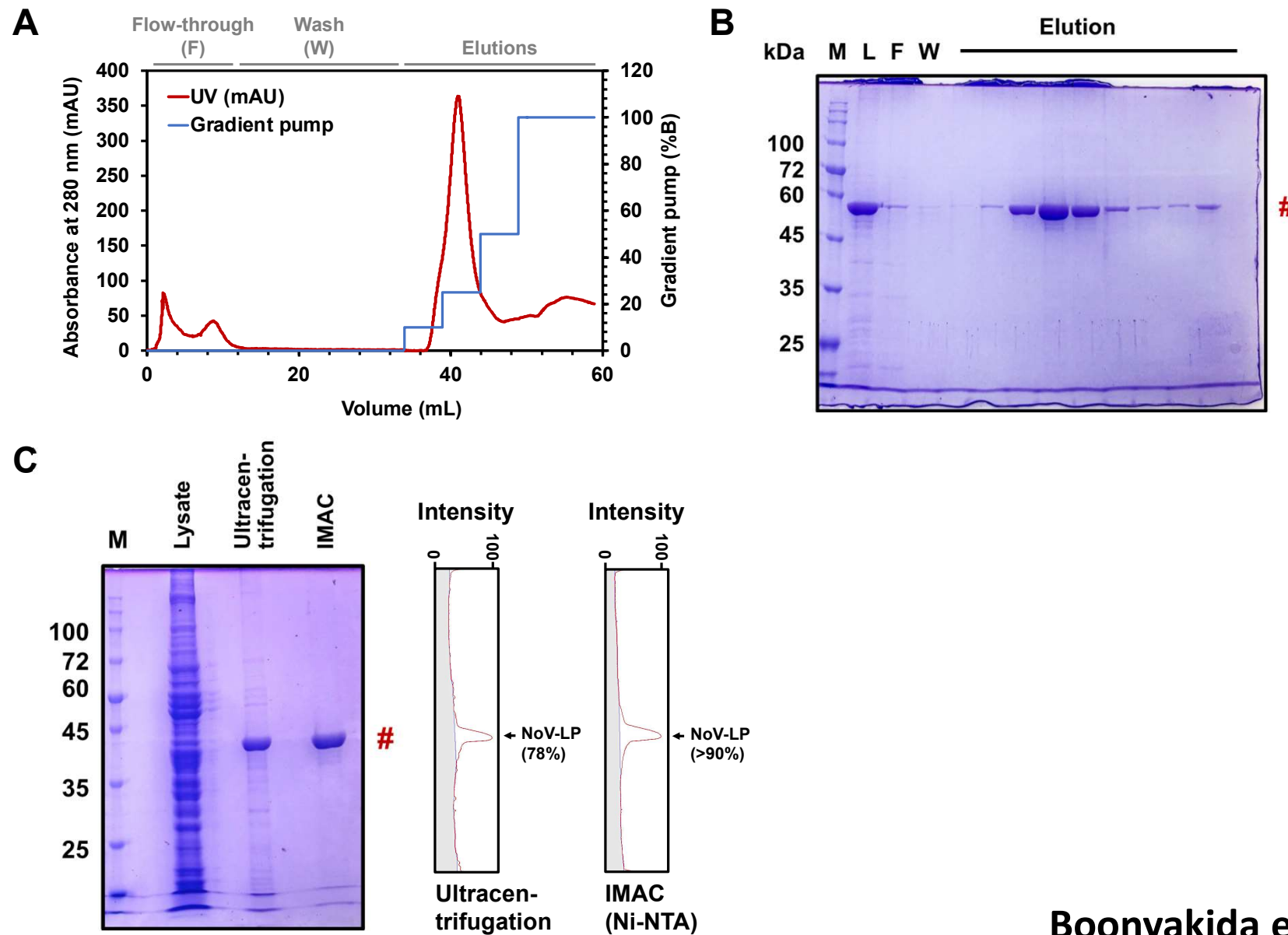


Fig. 2 Sucrose Grad. Cent.

Boonyakida et al. 2021



Boonyakida et al. 2021

Fig. 3

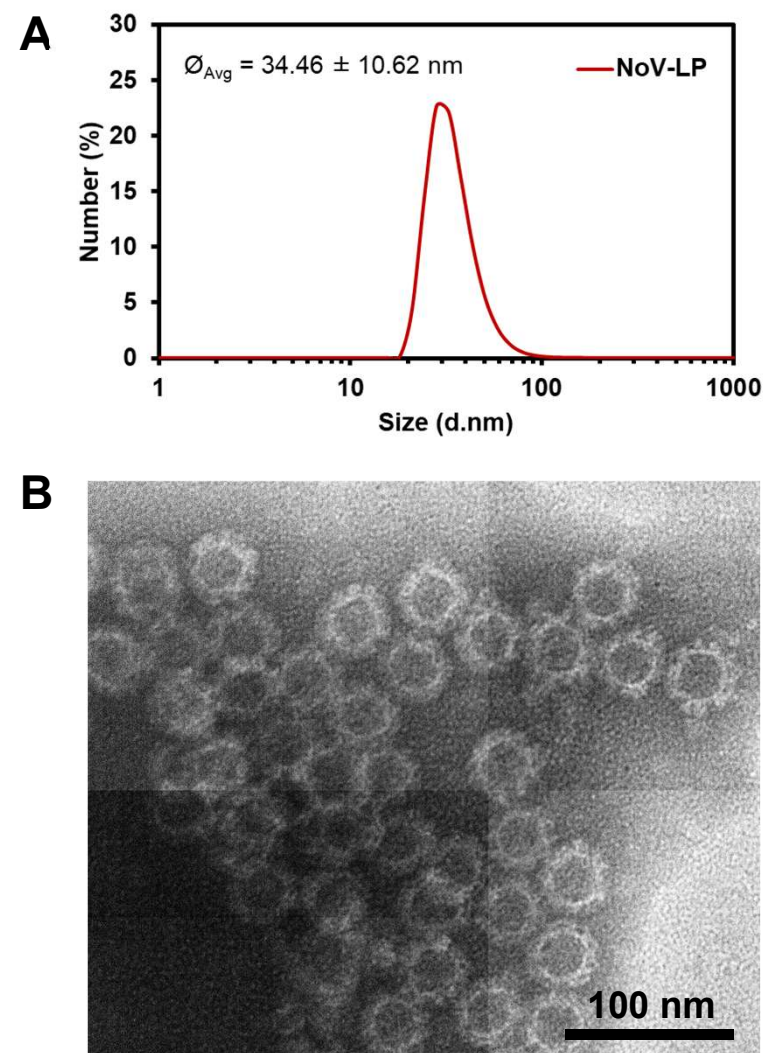


Fig. 4 DLS and TEM of NoV-LP after IMAC

Boonyakida et al. 2021

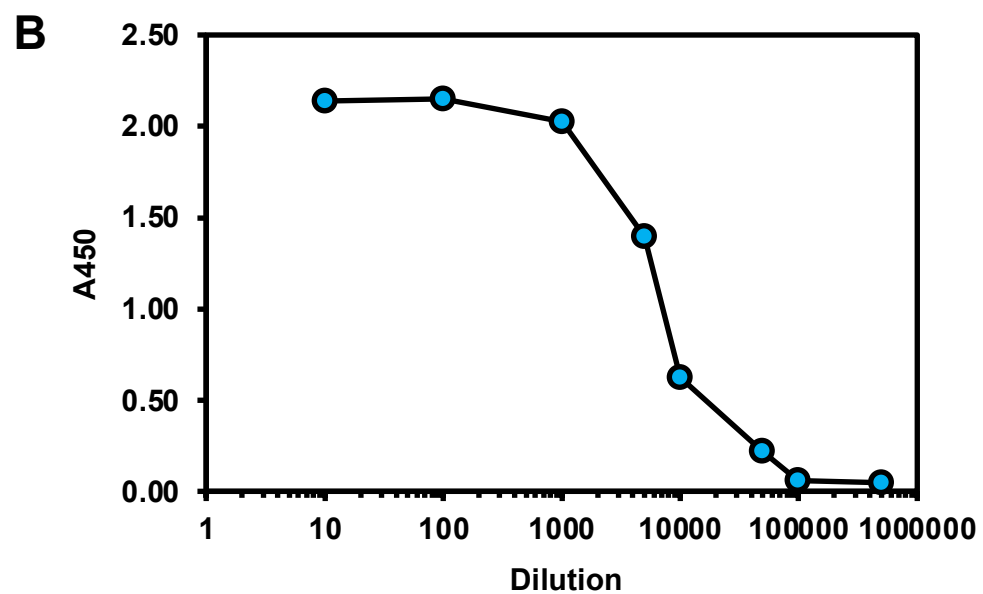
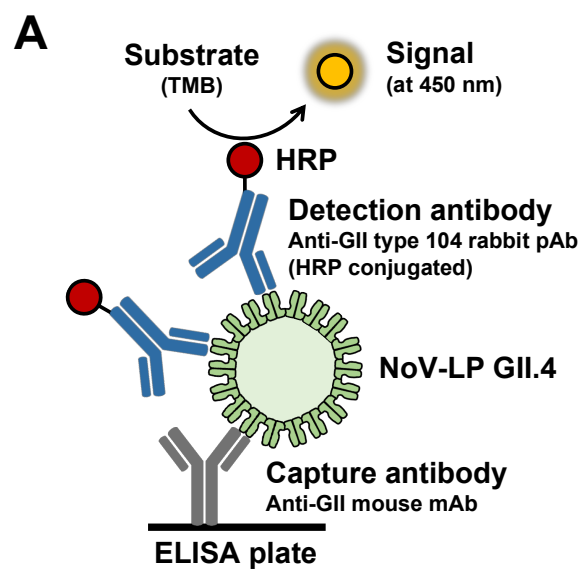


Fig. 5 ELISA of purified NoV-LP

Boonyakida et al. 2021

Supplementary information

Two-step purification of tag-free Norovirus-like particles from silkworm larvae (*Bombyx mori*)

Short running title: Expression and purification of norovirus-like particles from silkworm

Jirayu Boonyakida¹, [Doddy Irawan Setyo Utomo¹](#), [Fahmida Nasrin Soma²](#), Enoch Y. Park^{1,2,*}

¹ *Department of Bioscience, Graduate School of Science and Technology, Shizuoka University, 836 Ohya, Suruga-ku, Shizuoka 422-8529, Japan*

² *Research Institute of Green Science and Technology, Shizuoka University, 836 Ohya, Suruga-ku, Shizuoka 422-8529, Japan*

* Corresponding author.

E-mail address: park.enoch@shizuoka.ac.jp (E.Y. Park).

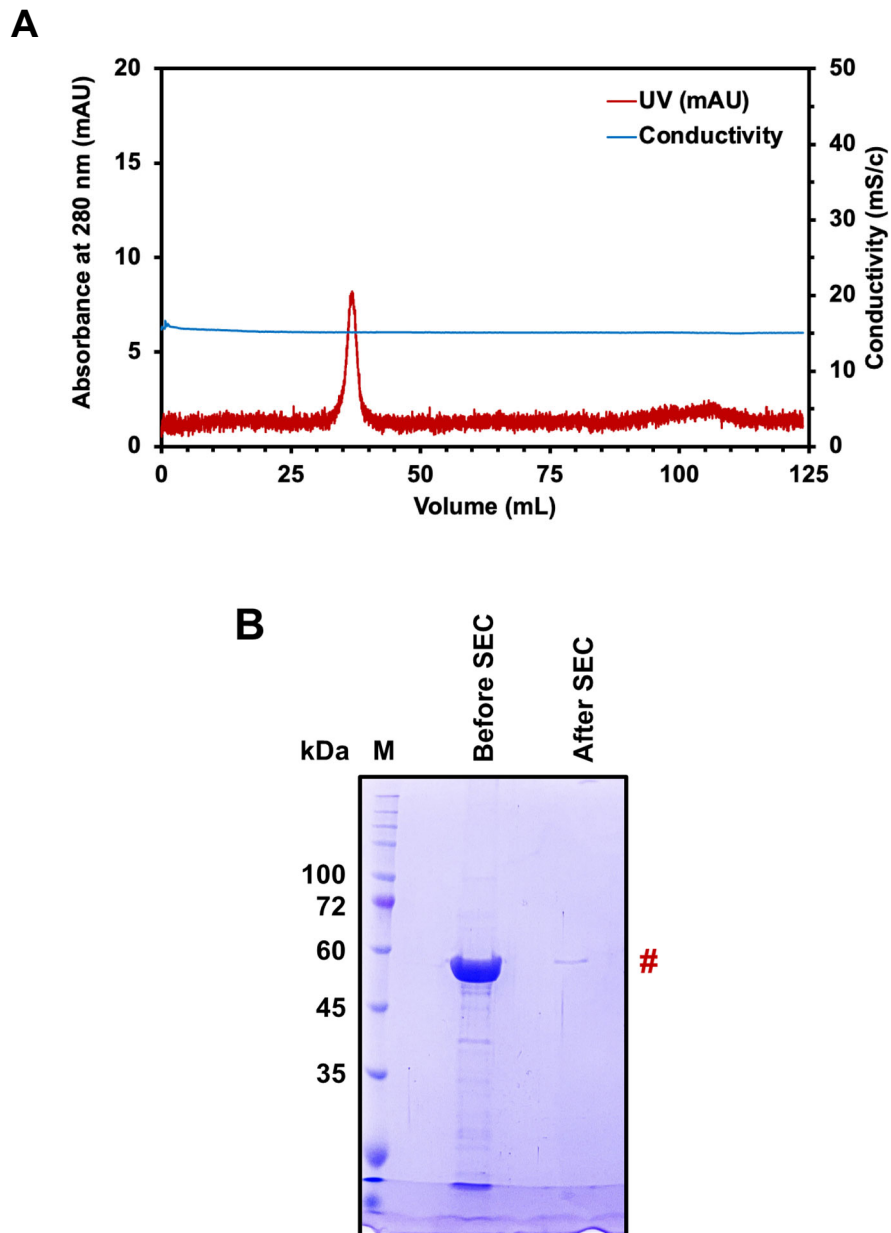


Figure S1. Size exclusion chromatographic (SEC) purification of VP1/NoV-LP after ultracentrifugation. The column used was HiPrep 16/60 Sephacryl S-200 High Resolution (HR). The flow rate was 1 mL/min during the entire run. **(A)** Chromatographic profile measured at 280 nm. Only one peak was observed between fractions 30-42. **(B)** SDS-PAGE/CBB staining of pooled fractions 30-42. After SEC purification, fractions 30-42

were pooled and concentrated using centrifugal concentrator, then separated on 12% SDS-PAGE gel comparing with the sample before SEC.